Neuroradiology (2004) 46: 435–443
DOI 10.1007/s00234-004-1191-5

M. Alemany Ripoll
A. Stenborg
P. Sonninen
A. Terent
R. Raininko

Detection and appearance of intraparenchymal haematomas of the brain at 1.5 T with spin-echo, FLAIR and GE sequences: poor relationship to the age of the haematoma

Received: 26 August 2003
Accepted: 23 November 2003
Published online: 11 May 2004

This work was presented at the XXVIII ESNR congress, in Istanbul, Turkey, September 2003

M. Alemany Ripoll (✉) · R. Raininko
Department of Radiology, Uppsala University Hospital, Uppsala, Sweden
E-mail: malemany@frs.seris.es
Tel.: +34-941-287235
Fax: +34-941-229153

A. Stenborg · A. Terent
Department of Internal Medicine, Uppsala University Hospital, Uppsala, Sweden

P. Sonninen
Department of Radiology, Turku University Hospital, Turku, Finland

Present address: M. Alemany Ripoll
Fundación Rioja Salud, Avda de Portugal no. 7, 6ª, 26001 Logroño, La Rioja, Spain

Abstract The specific appearance of blood related to time at T1- and T2-weighted spin-echo (SE) sequences is generally accepted; thus, these sequences are classically used for estimating the age of haematomas. Magnetic resonance imaging at 1.5 T, including T1- and T2-weighted SE fluid-attenuated inversion recovery (FLAIR) and T2*-weighted gradient-echo (GE) sequences, was performed on 82 intraparenchymal haematomas (IPHs) and 15 haemorrhagic infarcts (HIs) in order to analyse the appearance at different stages and with different sequences, and to investigate how reliably the age of hematomas can be estimated. The IPHs had been previously detected by CT, were spontaneous ($n=72$) or traumatic ($n=10$) in origin and were of different sizes (2 mm to 7 cm) and ages (from 7.5 h to 4 years after acute haemorrhagic event). The age of the lesion was calculated from the moment when clinical symptoms started or the traumatic event occurred. The 15 patients with HIs were patients with ischaemic stroke in whom there was either a suspicion of haemorrhagic transformation on CT, or haemorrhage was detected as an additional finding on MR performed for other indications. Patients with conditions that could affect the SI of blood, such as anticoagulant therapy or severe anaemia, were excluded. The signal intensity pattern of the lesions was analysed and related to their ages without prior knowledge of the clinical data. All lesions were detected with T2*-weighted GE. T1-weighted SE missed 13 haematomas and T2-weighted SE and FLAIR sequences missed five. Haemorrhagic transformation was missed in three infarcts by T1-, T2-weighted SE and FLAIR. The signal pattern on FLAIR was identical to that on T2-weighted SE. For all sequences, a wide variety of signal patterns, without a clear relationship to the age of the haematomas, was observed. There was a poor relationship between the real MR appearance of IPHs and the theoretical appearance on SE sequences. T2*-weighted GE was effective for detecting small bleedings but was not useful for estimating the age of a lesion. The FLAIR does not provide any more information than T2-weighted SE.

Keywords MRI · T2*-weighted GE sequence · Intracranial haematoma · Haemorrhagic infarct · Appearance · Detectability

Introduction

The MR recognition of blood can be challenging due to the highly variable appearance of haematomas, which depends on multiple factors, including sequence type, field strength and haematoma size and age. Intracranial haemorrhage (ICH) is a potentially life-threatening neurological condition that requires immediate diagnosis in order to apply a rapid and adequate treatment. In some instances, the therapy will change dramatically if the presence of blood is reported, for example, recognition of haemorrhage in acute stroke will contraindicate thrombolysis. The radiological evaluation of these patients is usually performed with computed tomography (CT), which is an excellent technique for depicting acute blood; however, the use of MRI is increasing due to its advantages over CT [1]. Although MR has not routinely substituted for CT, some diagnostic techniques that are not possible for the CT, such as diffusion-weighted imaging (DWI), are often needed to complete the evaluation of certain pathologies. The possibility of determining the age of a blood collection with the aid of its time-related MR appearance has been reported as another of the advantages of MRI [2]. The specific appearance of blood related to time at T1- and T2-weighted spin-echo (SE) sequences has been defined in the literature [3, 4] and is generally accepted; therefore, SE sequences are classically used for estimating the age of haematomas. The age of a lesion is of diagnostic importance because it influences the management of the patient: fresh and old bleedings require different treatment. There are also non-medical reasons, such as the confirmation of suspected child abuse through the depiction of intracranial haemorrhagic lesions at different stages.

However, in daily practice, discrepancies between the theoretical and real appearance of intracranial haematomas are common. We speculate that other sequences might help to estimate the age of these lesions. There are no systematic studies on the appearance of haematomas using FLAIR and gradient-echo (GE) sequences on patients.

The purpose of this study was to analyse the detection and MR appearance of intraparenchymal haematomas in the brain and haemorrhagic infarcts at different stages with T1- and T2-weighted SE, FLAIR and T2*-weighted GE sequences, and to compare the results with the age of the lesions. The aim was to increase knowledge about the complexity of the signal intensity (SI) of haematomas and provide information about the use of newer sequences for depict intraparenchymal bleedings.

Materials and methods

Magnetic resonance imaging was performed on 82 intraparenchymal haematomas, previously detected by CT in 75 patients. The intraparenchymal haematomas were spontaneous ($n=72$) or traumatic ($n=10$) in origin. Patients with conditions that could affect the SI of blood, such as anticoagulant therapy or severe anaemia, were excluded.

In addition, 15 patients with ischaemic stroke in whom either there was a suspicion of haemorrhagic transformation on CT, or haemorrhage was detected as an additional finding on MR performed for other indications, were studied. In 2 patients the haemorrhage was already seen on CT, although CT was uncertain for the presence of blood in 3 patients and negative in 11 patients.

The bleedings were of different sizes (2 mm to 7 cm) and ages (from 7.5 h to 4 years). The age of the lesion was calculated from the moment when the clinical symptoms started or the traumatic event occurred. The size was measured on SE sequences in three dimensions, and according to their maximal diameter, the haematomas were grouped into four categories as illustrated in Table 1. If the haematoma was not detected on SE images, the measurements were taken from GE images.

The MR technique and image analysis: MR examinations were performed at 1.5 T. The sequences and other imaging parameters are shown in Table 2. The MR images were analysed by an experienced radiologist blinded to the clinical data. For the purpose of this analysis, the haematomas were assumed to be layered, consisting of a rim, a bulk or body, and foci, and were surrounded by normal or oedematous brain tissue (Fig. 1). The SI of each layer was recorded

Table 1 Sizes of the intraparenchymal haematomas (IPH) and haemorrhagic infarcts (HI)

Size category	Maximal diameter	IPH ($n=82$)	HI ($n=15$)
Very small	≤ 1 cm	14	5
Small	1.1–2.5 cm	22	3
Medium	2.6–4 cm	33	3
Large	> 4 cm	13	4

Table 2 Imaging parameters. *TR* repetition time, *TE* echo time, *TI* inversion time, *w* weighted, *PD* proton density, *SE* spin echo, *GE* gradient echo, *FLAIR* fast fluid-attenuated inversion recovery

Sequences	TR/TE/TI (ms)	Flip angle	Plane
T1-w SE	500/14	Standard	Axial
PD-w SE	2300/16	Standard	Axial
T2-w SE	2300/120	Standard	Axial
FLAIR	10000/140/2000	Standard	Axial
T2*-w GE	500/14	30	Axial, coronal

and graded by comparison with normal brain or cerebrospinal fluid (CSF) (Table 3). Other features, such as inhomogeneity of the bulk, presence of fluid levels or other image characteristics, were also recorded. These characteristics were evaluated separately for the T1- and T2-weighted SE, FLAIR and T2*-weighted GE images.

After lesion analysis, the signal patterns were compared with the ages of the haemorrhages. The different ages were grouped into four stages as shown in Table 4.

All patients, except those studied for clinical indications, signed an informed consent. The study was carried out with the approval of the local ethics committee.

Results

The haematomas and haemorrhages in infarcts varied in size from a few millimetres to 7 cm (Table 1). The lesions were 1–2 mm larger when measured with the T2*-weighted GE than with SE sequences. The ages are presented in Table 4.

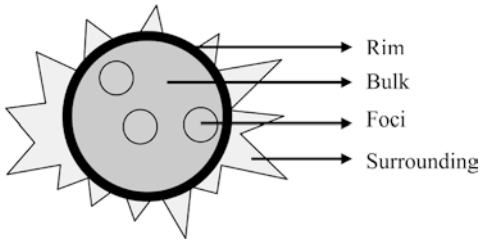

Fig. 1 Theoretical layers of the haematomas. The rim was defined as an external, usually thin area, well differentiated from the central part of the lesion in terms of signal intensity (SI), which separated the haematoma from surrounding normal or oedematous brain tissue. The bulk was defined as the main part of the haematoma, central to the rim. The foci were defined as any portion of the bulk that presented different SI, located either in the centre or more peripherally

Table 3 Grading scale for signal intensity analysis. → isointense, ↑ hyperintense, *WM* white matter, *GM* grey matter, *CSF* cerebrospinal fluid

T1-w images	T2-w images	FLAIR images	T2*-w images
→ to fat	→ to CSF	→ to fat	→ to CSF
↑ to WM	↑ to GM	↑ to GM	→ to GM
→ to WM	→ to GM	→ to GM	→ to WM
→ to GM	→ to WM	→ to WM	→ to fat
→ to CSF	→ to background	→ to CSF	→ to background

Table 4 Definition of the different stages. *IPH* intraparenchymal haematoma, *HI* haemorrhagic infarct

Age	Stage	No. of IPH	No. of HI
< 12 h	Hyperacute	1	0
12 h to 2 days	Acute	21	5
> 2–7 days	Early subacute	32	7
8 days to 1 month	Late subacute	10	3
> 1 month to years	Chronic	18	0
Total		82	15

T1-weighted SE

Detection and appearance of haematomas

Thirteen haematomas (16%), seven very small, two small and four of medium size, were not visualised on T1. Their ages varied from 14 h to 2.5 years. The only hyperacute haematoma in the series was large and showed a hypointense bulk with isointense rim surrounded by oedema. The acute haematomas, with ages comprising between 14 h and 2 days, presented a wide variation of SIs in the bulks and rims, occasionally also with hyperintense or hypointense foci. The first hyperintensities were seen in a 17-h-old lesion (Fig. 2). The haematomas aged from 2 days to 7 months, with the exception of five lesions, presented some areas of high SI, in the bulk, rim and/or foci, which helped to characterise them. Thirteen haematomas consisted of iso- or hypointense SIs without any hyperintensity: one in the hyperacute stage; eight in the acute stage; one in the subacute stage; and four in the chronic stage.

Detection and appearance of haemorrhagic infarcts

Three haemorrhages were not detected on T1, at 1, 2 and 3 days, respectively. Two of these lesions were very small and one small. Nine of the haemorrhages were characterised by the presence of hyperintense bulk or foci. The lesions were 1, 2 (two haemorrhages), 3, 6, 7, 9 and 19 days old. A variety of sizes were seen in this group. The remaining haemorrhages ($n = 3$) appeared iso- or hypointense to brain parenchyma, at 1 and 2.5 days, and at 3 weeks.

T2-weighted SE

Detection and appearance of haematomas

T2-weighted SE missed five haematomas (6%), three very small, one small and another of medium size, all of which were also missed by T1-weighted sequence. The

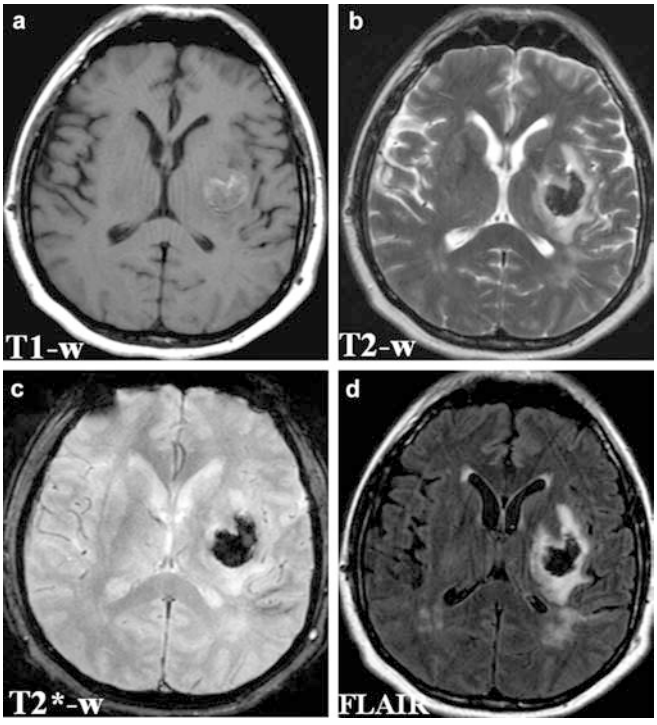

Fig. 2a–d A 17-h-old haematoma with T1- (**a**) and T2-weighted (**b**) SE sequences, T2*-weighted GE (**c**) and fluid-attenuated inversion recovery (FLAIR) (**d**). This lesion showed early hyperintense signal intensities on T1-weighted SE (**a**)

ages were 1.5 and 8 days, 3 months (two lesions) and 2.5 years. Low signal that helped to characterise the lesions could be detected at any age, including the hyperacute haematoma, which showed a hypointense rim. The most typical appearance was a high signal lesion with a dark rim, first at 7.5 h, and was the most common signal pattern from 7 days to 3 months.

Detection and appearance of haemorrhagic infarcts

Three of the haemorrhages were not detected on T2 (one was detected on T1), at 1, 2 and 3 days. Hypointense SI, characteristic of blood at this sequence, was depicted in 10 haemorrhagic infarcts (HIs). Stages varied from acute to chronic. Haemorrhage could not be characterised with this sequence in two cases that presented high SI, which occurred at 6 days and 3 weeks.

The SI patterns on FLAIR for haematomas and HIs were identical to those on T2-weighted SE, except for the serum collection seen in the periphery of four haematomas, which were partially suppressed by the FLAIR technique (Fig. 3). These results were obtained for all ages and sizes.

T2*-weighted GE

Detection and appearance of haematomas

T2*-weighted GE sequence detected all haematomas (100%). On five occasions (6%), only T2*-weighted GE sequence was capable of diagnosing haematomas that were invisible to the other sequences. The SI patterns found are presented in Table 5. There was no specific pattern indicating the age of the lesions (Fig. 4, 5, 6).

Detection and appearance of haemorrhagic infarcts

In 2 cases the haemorrhagic transformation of the infarcts was only detected with T2*-weighted GE. This sequence revealed a larger extent of haemorrhage in all patients (Fig. 7). In 3 patients the hyperintense areas on T1 were larger or did not correspond to the hypointensities on T2*-weighted GE (Fig. 8). These were interpreted as representing cortical laminar necrosis. All haemorrhages appeared markedly hypointense, and five, of different sizes, at 2, 3 (two haemorrhages), 7 and 9 days, also presented hyperintense foci.

All haematomas or haemorrhages, even the very small petechial lesions, presented some markedly hypointense areas on T2*-weighted GE; thus, identification with this sequence was easy.

The SI of the surrounding tissue characteristic for oedema (hypointense on T1-weighted SE and hyperintense on T2-weighted SE, FLAIR and T2*-weighted GE), progressively decreased in size over time. The hyperacute haematoma, 20 of 21 acute haematomas (95%), and 30 of 32 early subacute haematomas (94%), presented surrounding oedema. Hypointensities on T1, and hyperintensities on T2 in the surrounding tissue were found in 6 of 10 (60%) of late subacute haemato-

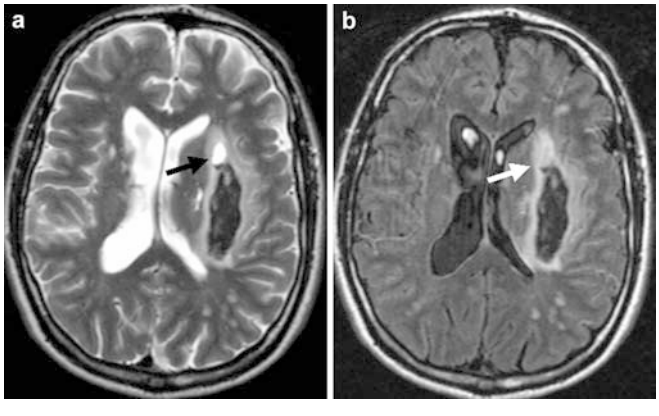

Fig. 3a, b A 2-day-old haematoma on T2-w SE (**a**) and FLAIR (**b**) sequences. A small hyperintense area in the ventral aspect of the haematoma, interpreted as serum collection (*black arrow*in **a**) was partially suppressed with FLAIR (*white arrow* in **b**). Otherwise, the signal intensity patterns are identical

Table 5 Signal intensity patterns of the haematomas on T2*-weighted GE. ↓↓ markedly hypointense, ↑↑ markedly hyperintense

SI patterns		Sizes	Ages
↓↓ homogeneous	40 (49%)	Any	Any age between 14h and 4yr
↑↑ bulk + ↓↓ rim (with or without dark foci)	22 (27%)	Small, medium or large	7.5 h 1 or 2 d 7 or 8 d after 3 weeks
Mixed SI always with ↓↓ rim	20 (24%)	Any	Any age between 24h and 2 months.

↓↓ = markedly hypointense, ↑↑ = markedly hyperintense

mas and in 8 of 18 (40%) of chronic haematomas. These changes were interpreted as secondary to gliosis. The same evolution was observed in the infarcts.

Discussion

T2*-weighted GE was able to depict the lesions missed by the other sequences and thus was the most sensitive sequence for detecting blood; nevertheless, this sequence did not help to estimate the age of the haematomas. T1-weighted SE missed 16% of haematomas and 20% of haemorrhages in infarcts. T2-weighted SE missed 6% of haematomas and 20% of haemorrhages in infarcts. The FLAIR did not provide any more information than T2-weighted SE. A wide variety of SI patterns was observed with all sequences, but no clear relationship to the age of the haematomas or haemorrhages was found.

To the authors' knowledge, this series contains the largest amount of material on the study of lesions with T2*-weighted GE and FLAIR sequences ever obtained.

The results revealed the high sensitivity of T2*-weighted GE to the presence of blood or blood products, even in cases of very small petechial lesions seen in haemorrhagic transformations of infarcts. On T2*-weighted GE the extent of haemorrhage in fresh infarcts was always greater than for other sequences. All haematomas and haemorrhages in this series presented

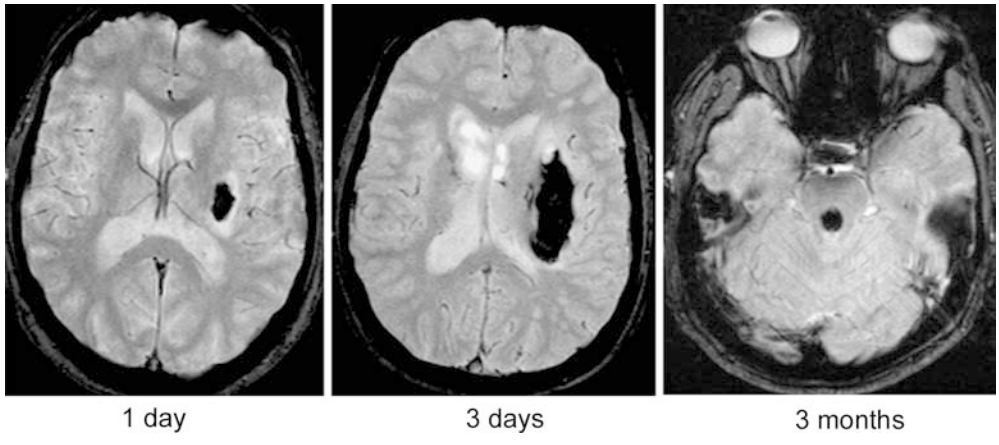

Fig. 4 Three examples of the most frequent pattern visualised on T2*-weighted GE: markedly hypointensity homogeneous or nearly homogeneous. Haematoma size and age vary. The chronic haematomas showing this pattern were all small or very small

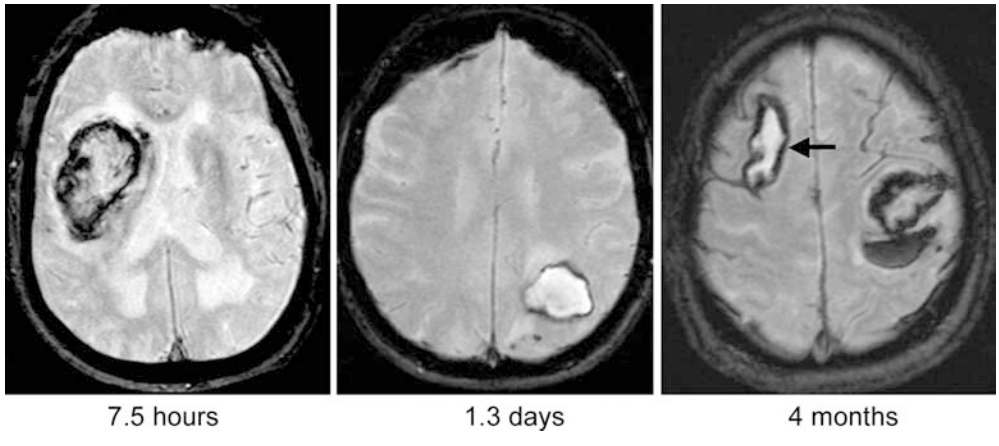

Fig. 5 Three examples of the second most frequent pattern on T2*-weighted GE: hyperintense bulk surrounded by a dark rim, with or without hypointense foci. In the image to the right, the 4-month-old haematoma is indicated with an *arrow*

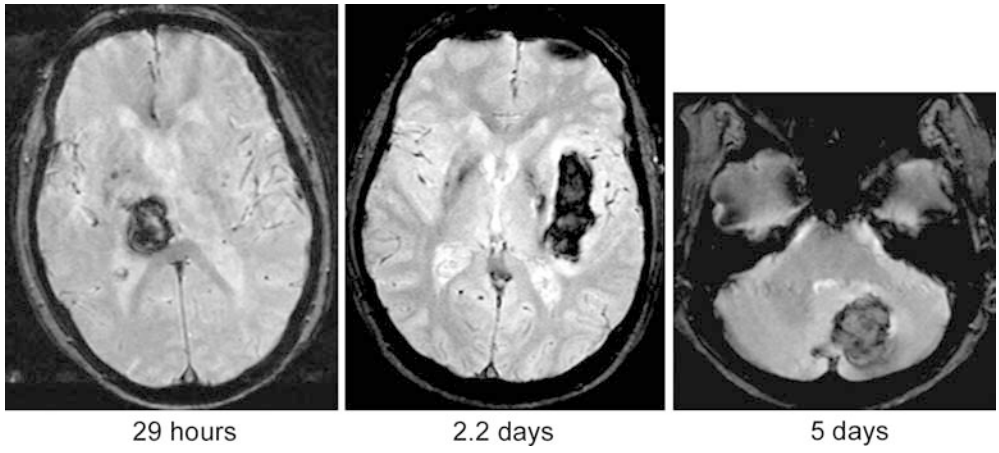

Fig. 6 Three examples of the third SI pattern visualised on T2*-weighted GE: a bulk with heterogeneous SIs surrounded by a dark rim. No predilection of sizes or ages was identified

some area or focus of marked signal loss that aided identification. Three patterns easily differentiable from each other, although not specific for the age of the lesions, were seen.

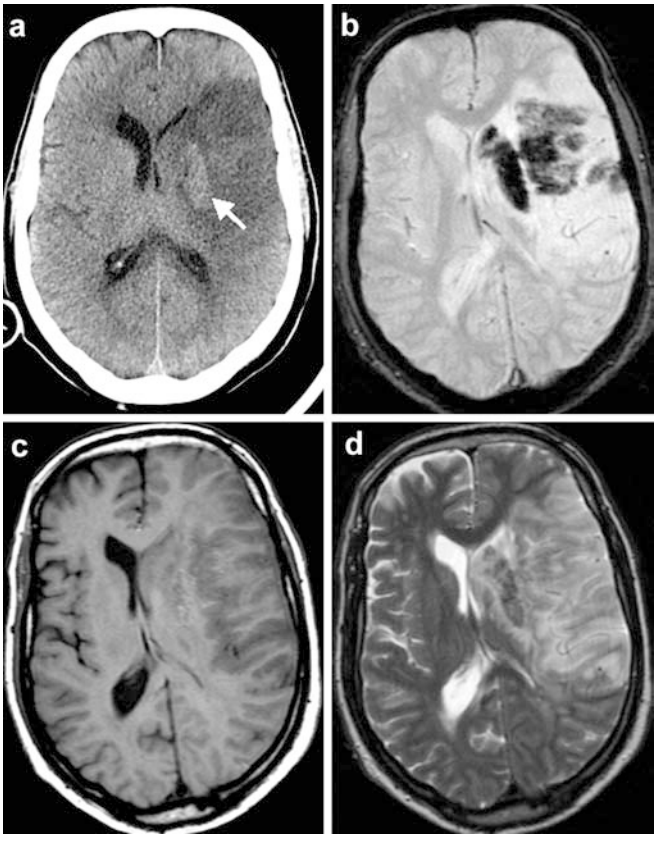

Fig. 7a–d Patient with an extensive infarct in the territory of the middle cerebral artery. The oval increased density in the left basal ganglia depicted on CT (*arrow*in **a**) could represent a spared lentiform nucleus. The MR images were obtained 3 days later. Haemorrhagic transformation is best depicted on T2*-weighted GE (*dark areas* in **b**). The haemorrhagic changes are underestimated on T1- (**c**) and T2-weighted (**d**) sequences

The limited number of descriptions of the appearance of haematomas on T2*-weighted GE sequences found in the literature [5, 6, 7] are generally for hyperacute lesions, due to clinical interest. In the present study, only one hyperacute haematoma was identified. It presented a hyperintense bulk with three to four hypointense peripheric foci and hypointense rim, and was large in size (6 cm in its maximum diameter). This appearance was in concordance with the previously mentioned studies.

The three different patterns identified in this series had a common feature: a dark rim or peripheric signal loss. This SI pattern has been explained by the ''boundary effect'', based on differences in magnetic susceptibility at the border of tissues, and by the very rapid deoxygenation of blood occurring in the interdigitation of blood and tissue at the periphery of the lesion. This last feature leads to rapid transition from diamagnetic oxyhaemoglobin to paramagnetic deoxyhaemoglobin at the blood–tissue interface [4]. The

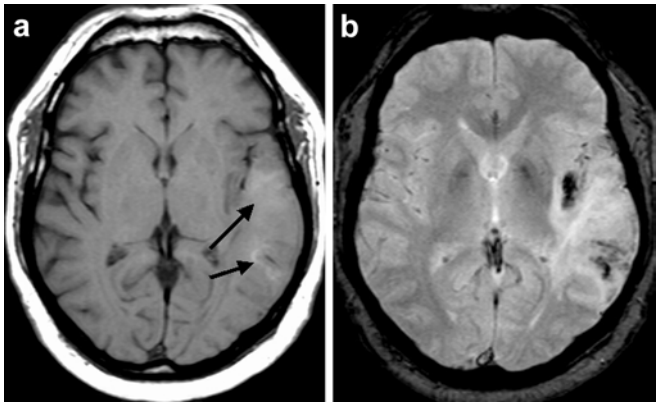

Fig. 8a, b Patient with a haemorrhagic infarct in the left temporal lobe. The hyperintense area seen on T1-weighted SE (*arrows* in **a**) is more extensive and does not correspond to the hypointensities on T2*-weighted GE (**b**). The hyperintensity on T1 most likely represents cortical laminar necrosis

resultant susceptibility effects in both cases causes rapid dephasing of proton spins with the consequent loss of SI on susceptibility-weighted sequences. Other authors have explained this SI pattern by the presence of perilesional haemosiderin [8], a well-known cause of signal loss in chronic haematomas. The presence of haemosiderin has been demonstrated with microscopy in experimental studies [9, 10], earliest at days 9–12 [9].

In a study on rats [11], haemosiderin was not detected within the first 24 h; thus, haemosiderin is an improbable cause of signal loss in hyperacute haematomas but may be an explanation for other stages. The haematomas presenting the most frequent pattern in this study, a markedly hypointense lesion, homogeneous or nearly homogeneous, probably had such a large amount of paramagnetic products that the only effect visible was the T2 effect, which would be the dominant contributor to the image.

In the second more frequent pattern, the bulk appeared hyperintense to brain parenchyma on T2*-weighted GE. This SI has also been described in the hyperacute stage [5, 6, 7]. A lack of deoxyhaemoglobin may explain the SI pattern: at this stage, the centre of the haematoma consists of fresh blood, with diamagnetic oxyhaemoglobin, and can be considered a proteinaceous solution; however, apart from the hyperacute haematoma, this pattern was also seen at 2, 5, 7, 9, 13 and 14 days; and at 1–4 months, when paramagnetic metabolites are supposed to have already appeared. The aetiology of this increased SI is unknown [5]. This hyperintense signal was interpreted as fluid collection without sufficient paramagnetic molecules to cause rapid proton dephase and thus signal loss.

The dark foci or mixed SIs seen at the hyperacute stage and at other stages in the present study were possibly due to clot formation; thus, signal loss reflected magnetic susceptibility differences between clotted and unclotted blood.

The three patterns discussed here were not specific for the age of the lesions. These results are in concordance with previous studies on rabbits: in a long-term follow-up of very small haematomas created in the brain parenchyma of the animals, fresh and old lesions could not be differentiated [12]. Some authors use the presence of surrounding oedema to differentiate acute from chronic haematomas [13]. The authors do not find this criterion to be useful, as high signal intensity in the surrounding tissue of chronic haematomas, probably due to gliosis, was common on T2-weighted images. That the three patterns could be identified at any stage may be due to differences in individual metabolic rates and to other unknown factors.

The hemorrhagic lesions appeared 1–3 mm larger when measured with susceptibility-weighted sequences. This has been explained by the so-called blooming effect [14] which consists in an apparent increase in haematoma size due to susceptibility effects in the border of two materials; however, this effect has not been detected in the hyperacute to subacute stages in experiments on rabbits [9, 15, 16], although it appeared in chronic stage [12]. Differences in the imaging parameters and haematoma size could be the explanation.

Table 6 Distribution of intraparenchymal hematomas (IPHs) of the present study in the categories described in the literature. ↑↑ markedly hyperintense, ↑ hyperintense, → isointense, ↓ hypointense, ↓↓ markedly hypointense

Categories according to [5] and [7]	T1-w SE	T2-w SE	No. of lesions	Ages of IPHs of present study with given pattern[b]
Hyperacute pattern	→ or ↓	↑	2	11 (1) days; 3 (1) months
Acute pattern	→ or ↓	↓↓	23	14 (2), 24 (1), 29 (1) and 30 (1) hours 3 (6), 4 (1), 5 (2) and 14 (1) days 1.5 (1), 2 (1), 9 (2) and 10 (1) months 1 (1), 2 (1) and 4 (1) years
Early subacute pattern	↑↑	↓↓	29	17 (1) and 23 (1) hours 1 (3), 1.5 (2), 2 (2), 2.5 (3), 3 (5), 3.5 (1), 4 (3), 4.5 (1), 5 (2), 7 (1) and 8 (1) days 3 (1), 4 (1) and 7 (1) months
Late subacute pattern	↑↑	↑↑	19	26 (1) and 30 (1) hours 2 (2), 4 (1), 5 (2), 6 (2), 7 (1), 8 (1), 9 (2) and 13 (1) days 1 (2), 3 (1), 3.5 (1) and 4 (1) months
Chronic pattern	→ or ↓	↓↓	23[a]	Same ages as in acute pattern
Other patterns			4	
Not visualized with T1- and T2-w SE sequences			5	1.4 (1) and 8 (1) days 3 (2) months 2.3 (1) years

[a]Same lesions as in acute pattern
[b]No. of lesions in parentheses

The FLAIR sequences for the diagnosis of haemorrhages have not been previously evaluated. This sequence did not provide any more information than T2-weighted SE sequence, probably because water is not a major component of haematomas at any stage. The SI of focal collections of serum seen in some lesions were partially suppressed with FLAIR.

In 3 patients with HI, hyperintense SI on T1-weighted SE in the infarcted area was seen, but the location did not correspond to or exceeded the size of the hypointensity on T2*-weighted GE in the same area. High T1 signal has been described in laminar cortical necrosis and demonstrated histopathologically to correspond to lipid-laden macrophages and mononuclear cells [9, 17, 18, 19]. Care must be taken in clinical practice to not diagnose haemorrhage incorrectly; thus, a combination of T1-weighted SE and T2*-weighted GE can help avoid misdiagnosis.

An important limitation to this study is the lack of histopathological verification that the so-called petechias really represent blood. This is especially true for the four small or very small haematomas and the two hemorrhagic transformations in infarcts, both very small, only detected by T2*-weighted GE and not seen by any of the other sequences. The foci of signal loss found in the present study have identical imaging characteristics to lesions analysed histopathologically in patients and in animals [9, 15, 20]; therefore, in the clinical context of these patients, these foci are believed to represent blood: the petechias were always seen in an infarcted area, making the diagnosis of hemorrhagic transformation reasonable. Nevertheless, previously present haematoma residuals [21] or other causes of signal loss on susceptibility-weighted sequences, such as deposits of calcium or metallic particles, cannot be completely excluded.

Computed tomography missed 13 of the 15 haemorrhages in infarcts in this series. The hemorrhagic transformation may have occurred in the time interval between the CT and the MRI, although in the majority of the cases the time difference between the two examinations was less than 2 days.

At present, many different staging systems for the evolution of haematomas can be found in the literature [3, 4, 22]. The nomenclature of the temporal stages of haematomas is somewhat arbitrary [4]. In addition, clinical dating is highly inaccurate, as the concepts of being ill and severity of illness are submitted to as many personal variations as human beings. The problems that arise when trying to report the age of intracranial blood increase as some bleeding episodes are clinically silent. The conceptual framework for understanding the MR appearance of cerebral haematomas on SE sequences has been summarised in multiple reviews [23, 24, 25, 26] based on in vitro studies, animal models and clinical observations [8, 20, 24, 25, 27, 28, 29, 30, 31]. The original model from Gomori et al. published in 1985 [29] emphasised the roles of iron associated with haemoglobin, oedema and gross structural changes in the haematoma, in determining relaxation mechanisms underlying the variable MR pattern. Based on these investigations, the specific time-related appearance of blood at T1- and T2-weighted SE has been defined and can be found in many texts. These concepts have been generally accepted and SE sequences are currently used to estimate the age of haematomas.

In this study the haematomas were grouped based on the time passed from symptom onset (Table 3). When the ages of the haematomas, which showed the same pattern as the expected for a particular stage, were compared (Table 6), discrepancy between the real and the expected ages was seen. In addition, 5% (4 of 82) of the haematomas could not be classified in any stage; thus, the ages of the lesions could not be estimated based on their appearance on SE sequences.

Conclusion

T2*-weighted GE is able to detect the haematomas of any age that are missed by other sequences and has also been demonstrated as effective in detecting small bleedings; however, T2*-weighted GE is not useful for estimating the age of the haematomas. The theoretical MR appearance of intracranial haematomas on SE sequences only partly corresponds to their real appearance. The FLAIR does not provide any more information than T2-weighted SE sequence.

Acknowledgements This work was supported by grants from the Swedish Medical Research Council No K2001-73X-13188-03A, K2001-73X-13188-03B, K2001-73X-13158-04A and K2001-73X-13158–04B, the Stroke Fund and the Selander Foundation. We thank M. Koisti for his help with data analysis and L. Johansson for discussions.

References

1. Schellinger PD, Jansen O, Fiebach JB, Hacke W, Sartor K (1999) A standardized MRI stroke protocol: comparison with CT in hyperacute intracerebral hemorrhage. Stroke 30:765–768
2. Broderick J, Adams H, Barsam W et al. (1999) Guidelines for the management of spontaneous intracerebral hemorrhage. Stroke 30:905–915
3. Parizel PM, Makkat S, Van Miert E, Van Goethem JW, van den Hauwe L, De Schepper AM (2001) Intracranial haemorrhage: principles of CT and MR interpretation. Eur Radiol 11:1770–1783
4. Atlas SW, Thulborn KR (2002) Intracranial haemorrhage. In: Atlas SW (ed) Magnetic resonance imaging of the brain and spine. Lippincott, Williams and Wilkins, Philadelphia, pp 773–832
5. Linfante I, LLinas R, Caplan L, Warach S (1999) MRI features of intracerebral hemorrhage within 2 hours from symptom onset. Stroke 30:2263–2267
6. Patel MR, Edelman RR, Warach S (1996) Detection of hyperacute primary intraparenchymal hemorrhage by magnetic resonance imaging. Stroke 27:2321–2324
7. Wiesmann M, Mayer T, Yousry I, Hamann G, Bruckmann H (2001) Detection of hyperacute parenchymal hemorrhage of the brain using echo-planar T2*-weighted and diffusion-weighted MRI. Eur Radiol 11:849–853
8. Atlas SW, Mark AS, Grossman RI, Gomori JM (1988) Intracranial hemorrhage: gradient-echo MR imaging at 1.5 T. Comparison with spin-echo imaging and clinical applications. Radiology 168:803–807
9. Alemany M, Gustafsson O, Siösteen B, Olsson Y, Raininko R (2002) MRI follow-up of small experimental intracranial haemorrhages from hyperacute to subacute phase. Acta Radiol 43:2–9
10. Thulborn KR, Sorensen AG, Kowall NW, McKee A, Lai A, McKinstry RC, Moore J, Rosen BR, Brady TJ (1990) The role of ferritin and hemosiderin in the MR appearance of cerebral hemorrhage: a histopathologic biochemical study in rats. AJNR 11:291–297
11. Atlas SW, Thulborn KR (1998) MR detection of hyperacute parenchymal hemorrhage of the brain. AJNR 19:1471–1477
12. Alemany M, Siösteen B, Hartman M, Raininko R (2003) MR detectability and appearance of small experimental intracranial haematomas at 0.5T and 1.5T: a follow-up study for 6–7 months. Acta Radiol 44:199–205
13. Nighoghossian N, Hermier M, Adeleine P, Blanc-Lassere K, DerexL, Honnorat J (2002) Old microbleeds are a potential risk factor for cerebral bleeding after ischemic stroke. A gradient-echo T2*-weighted brain MR study. Stroke 33:735–742
14. Young IR, Khenia S, Thomas DG, Davis CH, Gadian DG, Cox IJ, Ross BD, Bydder GM (1987) Clinical magnetic susceptibility mapping of the brain. J Comput Assist Tomogr 11:2–6
15. Alemany M, Raininko R (2002) Experimental intracerebral and subarachnoid/intraventricular haemorrhages: MR detectability at 0.5T and 1.5T. Acta Radiol 43:464–473
16. Gustafsson O, Rossitti S, Ericsson A, Raininko R (1999) MR imaging of experimentally induced intracranial hemorrhage in rabbits during the first 6 hours. Acta Radiol 40:360–368
17. Boyko OB, Burger PC, Shelburne JD, Ingram P (1992) Non-heme mechanisms for T1 shortening: pathologic, CT and MR elucidation. AJNR 13:1439–1445
18. Castillo M, Scatliff JH, Kwock L, Green JJ, Suzuki K, Chancellor K, Smith JK (1996) Postmortem MR imaging of lobar cerebral infarction with pathologic and in vivo correlation. Radiographics 16:241–250
19. Valanne L, Paetau A, Suomalainen A, Ketonen L, Pihko H (1996) Laminar cortical necrosis in MELAS syndrome: MR and neuropathological observations. Neuropediatrics 27:154–60
20. Del Bigio MR, Yan HJ, Buist R, Peeling J (1996) Experimental intracerebral hemorrhage in rats. Magnetic resonance imaging and histopathological correlates. Stroke 27:2312–2320
21. Roob G, Schmidt R, Kapeller P, Lechner A, Hartung H, Fazekas F (1999) MRI evidence of past cerebral microbleeds in a healthy elderly population. Neurology 52:991–994
22. Bradley WG Jr (1993) MR appearance of hemorrhage in the brain. Radiology 189:15–26
23. Barkovich AJ, Atlas SW (1988) Magnetic resonance imaging of intracranial hemorrhage. Radiol Clin North Am 16:801–820
24. Brooks RA, Giro G di, Patronas N (1989) MR imaging of cerebral hematomas at different field strengths: theory and applications. J Comput Assist Tomogr 13:194–206
25. Gomori JM, Grossman RI (1987) Head and neck hemorrhage. In: Kresel HY (ed) Magnetic resonance annual 1987. Raven Press, New York, pp 71–112
26. Thulborn KR, Brady TJ (1989) Iron in magnetic resonance imaging of cerebral hemorrhage. Magn Reson Q 5:23–28
27. Brooks RA, Brunetti A, Alger JR, Giro G di (1989) On the origin of paramagnetic inhomogeneity effects in blood. Magn Reson Med 12:241–248
28. Bryant RG, Marill K, Blackmore C, Francis C (1990) Magnetic relaxation in blood and blood clots. Magn Reson Med 13:133–144
29. Gomori JM, Grossman RI, Goldberg HI, Zimmerman RA, Bilaniuk LT (1985) Intracranial hematomas: imaging by high-field MR. Radiology 157:87–93
30. Gomori J, Grossman R, Yu-Ip C, Asakura T (1987) NMR relaxation times of blood: dependence on field strength, oxidation state and cell integrity. J Comput Assist Tomogr 11:684–690
31. Hackney DB, Atlas SW, Grossman RI et al. (1987) Subacute intracranial hemorrhage: contribution of spin density to appearance on spin echo MR images. Radiology 165:199–202